DFB Suppresses Obesity-Driven CRC Via Restricting Progenitor to Terminally Exhausted T Cell Differentiation

Yihua Xu
Southern Medical University
Hao Wang
Southern Medical University
Tao Wang
Naval Medical University
Chunhui Chen
The Second Affiliated Hospital of Guangzhou University of Chinese Medicine
Wanyu Yao
Southern Medical University
Ruibo Sun
Southern Medical University
Ye Ma
Southern Medical University
Qingyuan Zhang
Southern Medical University
Liyi Wu
Southern Medical University
Shanmei Zeng
Sun Yat-sen University First Affiliated Hospital
Xuegang Sun (sxg_smu@126.com)
Medical University School of Traditional Chinese Medicine

Research

Keywords: Dahuang Fuzi Baijiang decoction (DFB), T cell exhaustion, CCL2, Obesity, Colorectal cancer, Microenvironment

Posted Date: October 19th, 2021

DOI: https://doi.org/10.21203/rs.3.rs-952538/v1

Abstract

Background: Obesity contributes to about 30% incidence of colorectal cancer (CRC). Obese tumor microenvironment compromises anti-tumor immunity by eliciting exhausted T cells (Tex). Hypothesizing that Dahuang Fuzi Baijiang Decoction (DFB), a combined classical prescription from “Synopsis of Golden Chamber”, modulates the differentiation of tumor-infiltrating $CD8^+$ T cells

Methods: Our present study was to use transgenic *ob/ob* mice to examine the effects of DFB and to explore its novel mechanism on modulating the differentiation of tumor-infiltrating $CD8^+$ T cells.

Results: DFB regresses tumor growth in high-fat diet induced obese mice via expanding PD-1^{int}TIM3^- and restricting PD-1^{hi}TIM3^+ subset. TCF1 is highly expressed in PD-1^{int}TIM3^- subset but is absent in PD-1^{hi}TIM3^+ cells. We next confirm that progenitor PD-1^{int}TCF$^+$ cells robustly produce TNF and IFNγ while terminally differentiated PD-1^{int}TCF$^+$ cells have defects in generating TNF. With transgenic ob/ob mice, we find that DFB produces cooperative efficacy with anti-PD-1 (PD-1) by limiting PD-1^{hi}Tim3^+ subset and amplifying PD-1^{int}TCF$^+$ population. Finally, we identify that the differentiation from progenitor to terminal Tex is driven, at least in part, by CCL2. CCR2 inhibitor enhances the response to PD-1 by promoting the counts of progenitor Tex.

Conclusion: Altogether, DFB dampens CCL2 and preserves progenitor Tex in obese microenvironment to restrain CRC progression. These finds provide unambiguous evidence that traditional Chinese formula DFB can prevent tumor progression by modulating adaptive immunity and give rise to strong rationale for further clinical verification.

1. Background

Obesity is associated with 55% women cancers and 24% men cancers diagnosed [1]. Each 5-kg/m^2 BMI gaining can result in 13–18% increasing of colorectal cancer (CRC) risk [2]. Obesity contributes to 35.4% CRC cases in men and 20.8% in women [3]. Notably, about 40% of all cancer deaths are in large part associated with obesity [1]. Obesity represents a top risk factor and an independent prognostic variable of CRC.

CRC is an obesity-related cancer [4]. Cancer associated adipocyte secrets various adipokines, growth factors and sex-steroid hormones, including leptin, chemokine (C-C motif) ligand 2 (CCL2), insulin-like growth factor 1 (IGF-1), to create an immune privileged site. CCL2 is the pivotal chemokine that orchestrates the formation of immunosuppressive tumor microenvironment by empowering adipocytes to maintain chronic inflammatory responses, to skew the inflammatory cells to differentiate into immature phenotypes, as well as to increase T cell tolerance and dysfunction [5].

As a highly mutated cancer, CRC progressively losses its tumor antigen and MHC-1 contents until immune escape prevails [6]. Obesity tends to aid immune escape by conferring T cell population with

exhausted phenotype [7]. Exhausted T cells (Tex) are a discrete T cell subset characterized with progressively loss effector cytokines and impaired cytotoxicity [8]. Actually, Tex represent a hyporesponsive state which stem from adaptation to persistent antigen and chronic T cell receptors (TCR) stimulation [9].

Recently, it has been elegantly demonstrated that high-fat diet (HFD)-induced obesity dampens $CD8^+$ tumor-infiltrating lymphocytes (TILs) percentage and hampers their cytotoxicity [10]. In another study, obesity induces immune aging and promotes tumor growth across multiple strains and tumor types [11]. Obesity results in T cell exhaustion by increasing PD-1 expression and reducing interferon-γ (IFN-γ) and tumor necrosis factor-α (TNF-α) production in TILs. Surprisingly, obesity augments the efficacy of PD-1/PD-L1 blockade in various cancer patients and multiple tumor-bearing mice, suggest a controversial impact of obesity on cancers [11].

Dahuang Fuzi Baijiang decoction (DFB) is a combined classical prescription from “Synopsis of Golden Chamber” which has been praised as the ancestor of traditional Chinese medical formulary (Supplementary Table 2). Hypothesizing that combination of Dahuang Fuzi Decoction and Yiyi Fuzi Baijiang Powder ameliorates obesity induced T cell dysfunction, we test this idea with a series of *in vivo* experiments in tumor-bearing mice. Our results show that DFB expands progenitor Tex counts and maintain appropriate adaptive T cell response both in transgenic and diet-induced obese mice. These original findings would infuse novel meaning to the classical inheritance of traditional prescription and advance its clinical translation for tumor therapy.

2. Materials And Methods

2.1 Cell Lines

MC38 cell line (Heyuan Biotech. Shanghai) stably expressing luciferase (MC38-luc, generated via stable transduction with RediFect Red-Fluc lentivirus from PerkinElmer per manufacturer recommendations). Cells were cultured in normal DMEM without pyruvate supplemented with 10% FBS and 1% penicillin/streptomycin. Cells were cultured at 37℃ in a humidified 5% CO2 incubator.

2.2 Mice

8-week old *C57BL/6*, *C57BL/KS-ob* male mice were purchased from GemPharmatech Co., Ltd. For all experiments, 8-week old mice were assigned to Normal diet. All mouse colonies and experimental animals were maintained in the same animal facility at Southern Hospital of Southern Medical University and housed in specific pathogen-free conditions. All animals were used in accordance with animal care guidelines from the Southern Hospital Standing Committee on Animals and the National Institutes of Health. All mouse protocols were approved by the Southern Hospital Medical Area Standing Committee on Animals.

2.3 Mouse Tumor Models

Orthotopic tumor transplantation was performed as described previously [29–31]. Briefly, tumor tissue was prepared by injecting MC38-luc cells into the abdominal flank of mice. The tumor slices were transplanted into the ileocecal area of the mice in situ. Mice were sacrificed at humane endpoints or day 10-14 for tissue harvest. Animals were kept in a sterile environment and treatment with DFB (intragastric administration, i.g.) from the third day after surgery, daily, or αPD1 (intraperitoneal injection, i.p), CCR2-RA-[R] (i.p) every two days from the fifth day after surgery. Weight measurement every two days. The mice were euthanized at the end of the experiments. Tumor, serum, liver, and spleen were collected for further experiments.

2.4 Drugs preparation

The αPD1(In vivo Mab anti-mouse PD1) was purchased from BioX Cell(USA) and dissolved in PBS (200μg/kg/2d) .The CCR2 inhibitor CCR2-RA-[R] was purchased from MedChemExpress (USA) and dissolved in solvent (10% DMSO+90% corn oil) (5 mg/kg/2d) .

2.5 Tumor-Infiltrating Leukocyte Isolation

Weight 250 mg of tumor tissue, clean it repeatedly, and cut it into small pieces gently. Transfer the chopped tissue to a 15ml centrifuge tube and add 1ml PBS (protease inhibitor 1mM PMSF, 0.01mg/mL leupeptin, and 0.01mg/mL aprotinin). Gently shake the centrifuge tube, 100g, 4°C, centrifuge for 1 minute, aspirate the supernatant (mainly damaged tissue and cell debris) with a Pasteur pipette. Add 1ml of PBS to the precipitation sample and incubate it in a 37°C, 5% CO2 incubator for 1 hour. After the incubation, centrifuge at 1000g at 4°C for 3 minutes, take the supernatant, and discard the precipitate. Centrifuge at 2000g for 8 min at 4°C, take the supernatant, and discard the precipitate. Centrifuge at 20000g at 4°C for 30 min. Take the supernatant and discard the precipitate.

2.6 Enzyme-linked immunosorbent assay (ELISA)

Levels of TGFβ1, IL-6 and CCL2 in the tumor-Infiltrating leukocyte and serum were measured by ELISA Set(BD Biosciences, San Diego, CA) following its manufacturer's instructions. We used a microplate reader (Multiskan™ FC, ThermoFisher, MA, USA) to measure the absorbance at 450 nm.

2.7 Flow Cytometry

Primary mouse cells isolated from tumor were stained with fluorescent antibodies and analyzed by flow cytometry. Briefly, the tissue samples were first mechanically dissociated using a scalpel, then enzymatically dissociated in digestion medium (2 mg/ml Collagenase I (Sigma) and 0.2 mg/ml DNAse I (Sigma) in DMEM (Gibco)), incubated for 30 minutes at 37°C with gentle rocking. Red blood cells were removed from the cell suspension using red blood cell lysis buffer (Beyotime), and the cells were filtered using a 70-μm Flowmi tip strainer (VWR). Subsequent surface marker staining was performed in MACS buffer containing 1X PBS supplemented with 1% FBS and 2 mM EDTA. Intracellular staining for flow panels containing nuclear proteins was performed using the TCF1(RD system), TOX (Miltenyi)Transcription Factor Staining Buffer Set. For intracellular staining of cytoplasmic proteins, such as cytokines, the Fixation/Permeabilization Solution Kit (BD Biosciences) was used. Intracellular cytokine

staining was performed after a 6 hour stimulation with PMA (100 ng/mL) and ionomycin (500 ng/mL) in the presence of Golgi Stop at 37°C. Please see Key Resources Table for the fluorescently labeled antibodies used for staining. Antibodies targeting surface or intracellular proteins. Intracellular cytokine staining was performed after 5h *ex vivo* stimulation with GP33-41 peptide in the presence of Golgi Plug, Golgi Stop and anti-CD107a. After stimulation, cells were stained with surface antibodies, followed by fixation with Fixation/Permeabilization Buffer and then stained with intracellular antibodies for TNFα, IFNγ using Permeabilization Wash Buffer according to manufacturer's instructions. Data collection was performed on a BD FAC Symphony and analyzed using FlowJo v10.4.1.

2.8 Statistical analysis

Statistical analyses were performed using Graphpad Prism 8.0.2(GraphPad Software., San Diego, CA). All assays were repeated at least three times and data are presented as the mean ± standard deviation (SD). Differences between groups were calculated utilizing ANOVA or a Student's *t*-test for continuous variables. $P < 0.05$ was considered statistically significant.

3. Results

3.1. DFB suppress rapid growth of CRC in DIO mice by restricting terminal Tex

DFB, comprised of five commonly used herbs: Radix et Rhizoma Rhei (root or rhizome of perennial herbaceous plant Rheum palmatum L. Gansu, China), Radix Aconiti Lateralis Praeparata (root of perennial herbaceous plant Acontium carmichaeli Dehx. Sichuan, China), Herba Asari (root of Asarum sieboldii Miq. Liaoning, China), Semen Coicis (nut of Coix lachrhryma-jobi L.var.mayuen(Roman)Stapf. Guizhou, China), Herba Patriniae (entire plants of Patrinia scabiosaefolia Fisch. ex Link. and P. villose Juss. Hubei, China). The formula and amount of the prescription were listed in Table S2.

The raw herbs for DFB were purchased from Beijing Tongrentang Co. Ltd., China. The voucher specimens were deposited in the storage cabinet of Chinese traditional medicine of School of Traditional Chinese Medicine, Southern Medical University. A voucher specimen was deposited in the Herbarium of school of traditional Chinese medicine. These were mixed in the ratio of 12:6:30:15:3 (dry weight). Aqueous extracts of DFB were extracted at 80℃ by stirring it for 1 h using 10 volumes of distilled water (v/m). Then, we centrifuged the extract at 1,500×g at room temperature. To obtain the semisolid DFB solution, the supernatant was collected and subjected to condensation under reduced pressure of 70℃. The quality of DFB was controlled by HPLC analysis (Figure S2, Table S3). It was performed on Shimadzu LC-20A high-performance liquid chromatographic (HPLC) system (Shimadzu Co. Kyoto, Japan) by using a C18 column Shimadzu VP ODS (250 × 4.6 mm; particle size 5 μm, Japan). The mobile phases comprised eluent A (water) and eluent B (methanol). The gradient flow was as follows: 0.00–125.00 min, 20–90% B. The analysis was performed at a flow rate of 1.0 mL/min with PDA detection at 254 nm. The injection volume was 20 μL. Determination of Rhein(Pubchem CID:10168), Fuziline(Pubchem CID:14163819),

Asarinin(Pubchem CID:11869417), Coixol(Pubchem CID:10772), Quercetin(Pubchem CID:5280343) in DFB sample(Figure S1): as the five active compounds in Radix et Rhizoma Rhei, Radix Aconiti Lateralis Praeparata, Herba Asari, Semen Coicis and Herba Patriniae respectively.

To explore the suitable dosage of DFB, the size of murine colon adenocarcinoma (MC38-luciferase) (Supplementary Figure 3)xenografts was recorded every other day（Supplementary Figure 4A,C）. Both middle dosage and high dosage significantly restricted tumor growth, whereas the middle dosage showed better performance in regressing growth kinetics（Supplementary Figure 4D,E）. Hence, DFB middle dosage was chosen for subsequent research because of the best curative efficacy among the three different doses.

High fat diet (HFD)-fed obese mice closely mimicks the natural development of human obesity(Supplementary Table 1). We then monitored tumor growth in diet-induced obese mice (DIO, 60%-fat diet) versus control-diet mice (control, standard chow diet, SCD). DIO mice had a obvious increase of body weight at the end of 8 weeks（Figure 1B）. MC38 adenocarcinoma grew significantly faster in DIO mice as compared with control counterparts（Figure 1A）. DFB enormously limited the growth of MC38 tumors as demonstrated by luciferase-based biochemiluminescence imaging（Figure 1C）, suggested that DFB is highly effective in suppressing tumor growth even under a protumoral obese microenvironment.

We next studied the function of DFB on T cell phenotype in the obese microenvironment(Supplementary Figure 6A,B). Obesity slightly reduced the ratio of tumor-infiltrating $CD8^+$ T cells ($CD8^+$ TILs) in the tumor bed, whereas DFB significantly increased the recruitment of $CD8^+$ TILs（Figure 1D,F）. Specifically, HFD resulted in a markedly higher frequency PD-1^{hi}Tim3^+ $CD8^+$ TILs concomitant with an obvious decrease of PD-1^{int}Tim3^- subset as compared to control mice（Figure 1E,G,H）.PD-1^{hi}Tim3^+subset is generally defined as terminally differentiated exhausted T cells whereas intermediate expression of PD-1 (PD-1^{int}) and co-existence of TCF-1 confer Tex with stem cell-like properties [9, 12]. DFB increased the number of PD-1^{int} subset and lowered PD-1^{hi}Tim3^+ cells in the tumor. Taken together, DFB suppresses HFD-accelerated tumor progression by reserving PD-1^{int} subset and decreasing Tex counts.

3.2 TOX and TCF1 control Tex differentiation status

Terminally differentiated Tex is the driving force to form immunosuppressive microenvironment, whereas progenitor Tex subset is critical for generating response to PD-1 blockade [13–15]. To characterize the differentiation state of the two subsets, we sorted and analyzed transcription activity of TCF1 and thymocyte selection-associated high mobility group box (TOX)(Supplementary Figure 6C). PD-1^{int}TIM3^- cells are characterized by strong expression of TCF1 which is absent in PD-1^{hi}Tim3^+ cells（Figure 2A,C）. These TCF1^+PD-1^{int} progenitor cells can expand and yield terminal exhausted PD-1^{hi}Tim3^+ cells. We observed a highly expression of TOX in the PD-1^{hi}Tim3^+ subset（Figure 2A,D）.TOX transcriptionally activates co-inhibitory receptor gene Pdcd1 and stimulates the transcription of Tcf7 which is the encoding gene for TCF1. We also noticed a overlap of TOX and TCF1 expression in TCF1^+PD-1^{int} subset,

suggested that TOX may act upstream of TCF1 to drive the differentiation from progenitor to terminal Tex.

As Tex progressively lose its effector function in a hierarchical pattern, we examined the alterations of effector cytokines with an *ex vivo* experiment. The sorted TCF1^{+}PD-1^{int} and PD-1^{hi}Tim3^{+} cells were stimulated with CD3 and CD28 antibody (Supplementary Figure 6C). TCF1^{+}PD-1^{int} cells displayed robust ability to produce TNF and IFNγ. However, PD-1^{hi}Tim3^{+} exhibited defects in generating IFN-γ while showed residue competence to produce TNF（Figure 2E,F）. Loss of IFNγ has been considered occurring at the late stage of exhaustion [12], our results suggested that the cytotoxity defect in PD-1^{hi}Tim3^{+} cells is corresponding to the terminally exhausted state（Figure 2E,G）. These distinct fingerprints of Tex suggested that TOX and TCF1 drive the evolution between progenitor and terminal Tex which determine the exhausted status and their response to checkpoint blockade.

3.3 DFB reserves progenitor Tex to elicit immune response to αPD-1

As PD-1^{int}TCF-1^{+} progenitor TILs are poised to respond to PD-1 blockade, we reasoned that DFB might coordinate anti-PD-1 (αPD-1) response by modulating PD-1 expression in CD8^{+} T cells. *Ob/ob* mice carry a spontaneous mutation at the leptin locus which lead to obesity, hyperglycemia, and elevated plasma insulin. *Ob/ob* mice exhibited visible obese with elevated body weight and abdominal circumference(Supplementary Figure 7A,B). Mirroring the protumorigenic activity of DIO, *ob/ob* phenotype drastically accelerated MC38 tumor growth as compared to its corresponding *C57BL/6J* background（Supplementary Figure 6A,C）. DFB not only moderately attenuated tumor growth, but displayed prominent cooperative efficacy in limiting tumor size in *ob/ob* mice（Supplementary Figure 3B,C）.

To investigate whether reduced growth rates of tumors by DFB was due to control by T cells, we re-genotyped the T cells in the tumor with PD-1 and TIM3(Supplementary Figure 6A,B). DFB augmented the number of CD8^{+} T cells and synergized the effects of αPD-1（Figure 3D,F）. As expected, *ob/ob* mice increased the percentage of PD-1^{hi}Tim3^{+} cells, corresponding to an reduction of of PD-1^{int} cells（Figure 3E,G,H）. DFB substantially decreased the ratio of terminal PD-1^{hi}Tim3^{+} Tex to ameliorate the immunosuppressive condition. It also increased the number of PD-1^{int} T cells that serve to respond to αPD-1 immunotherapy. Together, DFB curbs the tumor growth by limiting PD-1^{hi}Tim3^{+} subset and amplifying PD-1^{int} population to enhance the efficacy of PD-1 checkpoint blockade.

3.4 DFB reduces tumor interstitial and serum CCL2 production

Obesity has been demonstrated to induce a chronic, low-grade inflammatory status with increased adipokines, such as IL-6, TGF-β, leptin, TNF-α, as well as elevated levels of CCL2. *Ob/ob* genotype

elevated interstitial IL-6 production, while had no obvious impact on TGF-β secretion as compared to age-matched wild type mice(Figure 4A,D). DFB substantially depressed tumor interstitial IL-6 content whereas displayed no synergistic effects with αPD-1 on IL-6 level（Figure 4B,E）.

CCL2, which is symbolically presented at high levels in obesity, gives rise to immune evasion through PD-1 signaling [16]. We first accessed the effects of DFB on CCL2 in *ob/ob* mice. DFB reversed obesity-raised stromal CCL2 content. Although, αPD-1 alone can not lowered CCL2 secretion, DFB helped αPD-1 inhibitor to reduce stromal CCL2 level(Figure 4C,F). We next evaluated the impact of DFB in DIO mice and observed a remarkably similar pattern. DFB attenuated interstitial CCL2 content in HFD feeding obese mice. Additionally, we also measured the alteration of serum CCL2 contents. As expected, either DFB and αPD-1, and the two together decreased serum CCL2 elevation which is induce by obese background. Collectively, DFB dampens obesity-driven tumor interstitial and serum CCL2 production both in DIO and transgenic obese mice.

3.5 CCR2 inhibitor blocks shift from progenitor Tex to terminal Tex

As elevated CCL2 expression drives PD-1 inhibitor-resistance [17] and CCR2 antagonism enhances tumor response to αPD-1 monotherapy [18], we then tested if CCL2-CCR2 axis contributes to Tex differentiation with a specific inhibitor CCR2-RA-[R]. As we saw earlier, MC38 tumor growth was accelerated in *ob/ob* mice compared with control C57BL6/J mice(Figure 5A,B). CCR2 inhibitor restrained tumor growth and increased $CD8^+$ T cell infiltration（Figure 5C,E）.

We also observed an reduction of progenitor PD-1^{int} number in *ob/ob* mice as compared to their wild type counterparts. Importantly, CCR2 inhibitor enhanced the percentage of progenitor PD-1^{int} cells, and also expanded this subset when combined with αPD-1 immunotherapy(Figure 5D,F,G).Corresponding to its protumor phenotype, *ob/ob* mice also increased the ratio of terminal PD-$1^{hi}$$TIM3^+$ $CD8^+$ TILs, whereas CCR2 inhibitor reduced the counts of this subset. Hence, obese enhance tumor interstitial CCL2 to facilitate the differentiation from progenitor to terminal Tex. DFB exerts it antitumor activity through disturbing CCL2/CCR2 mediated terminal T cell exhaustion [18]. Altogether, DFB decreases obesity-driven CCL2 secretion and reverses the Tex differentiation shift to regress CRC progression.

4. Discussion

Obesity boosts tumor infiltrating lymphocytes entering an exhausted state. T cell exhaustion represents a compromise to continuous antigen stimulation which allows T cells to control tumor growth without causing detrimental immunological pathology. However, cancer cells have hijacked the exhaustion tactics during evolution, encouraging the adaptive immune system to ‘tolerate’ them so as to gain the survival allowance. The ‘host-pathogen stalemate’ during obesity reveals that the ‘anergy’-like hyporesponsive state of T cell and chronic inflammation can be coupled [9]. So, DFB might suppress obesity-associated

incidence of CRC via ameliorating adaptive state of T cell hyporesponsiveness and dampening low-grade inflammation [9] .

Of particular note, DFB increases the infiltration of $PD1^{int}TCF1^{+}$ subset which can be ascribe to progenitor/stem-like exhausted T cells [22].The specific pool of exhausted T cells retain partial protective capability once reinvigorated by blockade of the PD1 pathway [21]. Importantly, these progenitor cells hold potential to proliferate and to yield terminally differentiated Tex. DFB inhibits the shift of progenitor exhausted T cells to terminally differentiated T cells and augments effects PD-1 checkpoint blockade. So, DFB provides synergistic therapeutic benefit with checkpoint blockade to enhance the enhancer in tumor immunity [18].

The hyperplasia and hypertrophy of adipocytes in obesity trigger chronic inflammation by increasing the secretion of CCL2 [24]. It has been well demonstrated that CCL2/CCR2 axis enhance tumor progression by amplifying the recruitment of myeloid-derived suppressor cells (MDSCs) and metastasis-promoting monocytes [25, 26]. Our results give additional evidence that CCL2 impose T cells differentiating into a terminally exhausted phenotype to permit and augment the progression of CRC.

CCR2 antagonism promotes tumor response to PD-1 inhibitor in multiple cancer type [18, 27], indicated that $CCR2^{+}CD8^{+}$ subset may be immunosuppressive. DFB reverses the CCL2 production in the obese microenvironment and holds Tex back into a progenitor state. So, targeting CCL2/CCR2 might be a suitable strategy in rescuing terminally T cell exhaustion.

5. Conclusion

Altogether, DFB dampens CCL2 and preserves progenitor Tex in obese microenvironment to restrain CRC progression(Figure 6). Obesity enhances tumor progression by raising CCL2 secretion which recruits terminally exhausted T cells to establish a healthy-Qi deficient microenvironment. DFB strengthens healthy-Qi and eliminates cancerous lesions by restricting CCL2/CCR2 mediated exhausted T cell recruitment. DFB also inhibits the polarization of progenitor T cells to terminal exhausted T cells. The preservation of progenitor Tex is indispensable for the response to PD-1 checkpoint blockade [29]. Taken together, our outcomes pave an novel avenue to use classic prescriptions to cure cancerous disease through regulating adaptive immunology. Although the two constituent formula of DFB have been used for thousands of years, the immunomodulatory properties of DFB still need further confirmation from clinical practice.

Declarations

Ethics approval and consent to participate

All animal care and procedures were in accordance with China and Nanfang hospital policies for health and well-being.

Consent for publication

Not applicable.

Availability of data and material

All data generated or analyzed during this study are included in this published article.

Competing interests

The authors declare that they have no competing interests.

Funding

This work was supported by the National Science Foundation of China (81974554, 81774172, 81904075), Key-Area Research and Development Program of Guangdong Province, Modernization of Chinese medicine in Lingnan (2020B1111100011), Planned Science Technology Project of Guangzhou (202002030111).

Authors' contributions

XYH participated in the design of the study, carried out the animal experiment and drafted the manuscript. WH participated in the animal experiment, performed the statistical analysis. WT carried out the immunoassays. CCH conceived of the study, and participated in its design. YWY participated in the animal experiment and coordination and helped to draft the manuscript. SRB participated in the animal experiment. MY participated in submission. ZQY, WLY, ZSM coordination and helped to draft the manuscript. All authors read and approved the final manuscript.

Acknowledgements

Not applicable.

References

1. Steele CB, Thomas CC, Henley SJ, Massetti GM, Galuska DA, Agurs-Collins T, et al. Vital Signs: Trends in Incidence of Cancers Associated with Overweight and Obesity - United States, 2005-2014. MMWR Morb Mortal Wkly Rep. 2017;66(39):1052–58.
2. Eheman C, Henley SJ, Ballard-Barbash R, Jacobs EJ, Schymura MJ, Noone AM, et al. Annual Report to the Nation on the status of cancer, 1975-2008, featuring cancers associated with excess weight and lack of sufficient physical activity. *Cancer-Am Cancer Soc*. 2012;118(9):2338-66.
3. Calle EE, Kaaks R. Overweight, obesity and cancer: epidemiological evidence and proposed mechanisms. Nat Rev Cancer. 2004;4(8):579–91.
4. Bardou M, Barkun AN, Martel M. Obesity and colorectal cancer. Gut. 2013;62(6):933–47.

5. Kanneganti TD, Dixit VD. Immunological complications of obesity. Nat Immunol. 2012;13(8):707–12.
6. Woodall MJ, Neumann S, Campbell K, Pattison ST, Young SL. The Effects of Obesity on Anti-Cancer Immunity and Cancer Immunotherapy. *Cancers (Basel)*. 2020;12(5).
7. Xie Q, Ding J, Chen Y. Role of CD8(+) T lymphocyte cells: Interplay with stromal cells in tumor microenvironment. Acta Pharm Sin B. 2021;11(6):1365–78.
8. Yang Y, Liu F, Liu W, Ma M, Gao J, Lu Y, et al. Analysis of single-cell RNAseq identifies transitional states of T cells associated with hepatocellular carcinoma. Clin Transl Med. 2020;10(3):e133.
9. Blank CU, Haining WN, Held W, Hogan PG, Kallies A, Lugli E, et al. Defining 'T cell exhaustion'. Nat Rev Immunol. 2019;19(11):665–74.
10. Ringel AE, Drijvers JM, Baker GJ, Catozzi A, Garcia-Canaveras JC, Gassaway BM, et al. Obesity Shapes Metabolism in the Tumor Microenvironment to Suppress Anti-Tumor Immunity. Cell. 2020;183(7):1848–66.e26.
11. Wang Z, Aguilar EG, Luna JI, Dunai C, Khuat LT, Le CT, et al. Paradoxical effects of obesity on T cell function during tumor progression and PD-1 checkpoint blockade. Nat Med. 2019;25(1):141–51.
12. Viana I, Roussel S, Defrene J, Lima EM, Barabe F, Bertrand N. Innate and adaptive immune responses toward nanomedicines. Acta Pharm Sin B. 2021;11(4):852–70.
13. McLane LM, Abdel-Hakeem MS, Wherry EJ. CD8 T Cell Exhaustion During Chronic Viral Infection and Cancer. Annu Rev Immunol. 2019;37:457–95.
14. Dammeijer F, van Gulijk M, Mulder EE, Lukkes M, Klaase L, van den Bosch T, et al. The PD-1/PD-L1-Checkpoint Restrains T cell Immunity in Tumor-Draining Lymph Nodes. Cancer Cell. 2020;38(5):685–700.e8.
15. Miller BC, Sen DR, Al AR, Bi K, Virkud YV, LaFleur MW, et al. Subsets of exhausted CD8(+) T cells differentially mediate tumor control and respond to checkpoint blockade. Nat Immunol. 2019;20(3):326–36.
16. Sakuishi K, Apetoh L, Sullivan JM, Blazar BR, Kuchroo VK, Anderson AC. Targeting Tim-3 and PD-1 pathways to reverse T cell exhaustion and restore anti-tumor immunity. J Exp Med. 2010;207(10):2187–94.
17. Yang H, Zhang Q, Xu M, Wang L, Chen X, Feng Y, et al. CCL2-CCR2 axis recruits tumor associated macrophages to induce immune evasion through PD-1 signaling in esophageal carcinogenesis. Mol Cancer. 2020;19(1):41.
18. Tu MM, Abdel-Hafiz HA, Jones RT, Jean A, Hoff KJ, Duex JE, et al. Inhibition of the CCL2 receptor, CCR2, enhances tumor response to immune checkpoint therapy. Commun Biol. 2020;3(1):720.
19. Chen X, Pan X, Zhang W, Guo H, Cheng S, He Q, et al. Epigenetic strategies synergize with PD-L1/PD-1 targeted cancer immunotherapies to enhance antitumor responses. Acta Pharm Sin B. 2020;10(5):723–33.
20. Sinicrope FA, Foster NR, Sargent DJ, O'Connell MJ, Rankin C. Obesity is an independent prognostic variable in colon cancer survivors. Clin Cancer Res. 2010;16(6):1884–93.

21. Chen Z, Ji Z, Ngiow SF, Manne S, Cai Z, Huang AC, et al. TCF-1-Centered Transcriptional Network Drives an Effector versus Exhausted CD8 T Cell-Fate Decision. Immunity. 2019;51(5):840–55.e5.
22. Beltra JC, Manne S, Abdel-Hakeem MS, Kurachi M, Giles JR, Chen Z, et al. Developmental Relationships of Four Exhausted CD8(+) T Cell Subsets Reveals Underlying Transcriptional and Epigenetic Landscape Control Mechanisms. Immunity. 2020;52(5):825–41.e8.
23. Pauken KE, Wherry EJ. SnapShot: T Cell Exhaustion. Cell. 2015;163(4):1038.e1.
24. Gu Y, Liu Y, Cao X. Evolving strategies for tumor immunotherapy: enhancing the enhancer and suppressing the suppressor. Natl Sci Rev. 2015;4(2):161–3.
25. Catalan V, Gomez-Ambrosi J, Rodriguez A, Ramirez B, Ortega VA, Hernandez-Lizoain JL, et al. IL-32alpha-induced inflammation constitutes a link between obesity and colon cancer. Oncoimmunology. 2017;6(7):e1328338.
26. Hartwig T, Montinaro A, von Karstedt S, Sevko A, Surinova S, Chakravarthy A, et al. The TRAIL-Induced Cancer Secretome Promotes a Tumor-Supportive Immune Microenvironment via CCR2. Mol Cell. 2017;65(4):730–42.e5.
27. Yang Y, Li L, Xu C, Wang Y, Wang Z, Chen M, Jiang Z, Pan J, Yang C, Li X, et al. Cross-talk between the gut microbiota and monocyte-like macrophages mediates an inflammatory response to promote colitis-associated tumourigenesis. Gut. 2020;70:1495–506.
28. Shi L, Wang J, Ding N, Zhang Y, Zhu Y, Dong S, et al. Inflammation induced by incomplete radiofrequency ablation accelerates tumor progression and hinders PD-1 immunotherapy. Nat Commun. 2019;10(1):5421.
29. Miller BC, Sen DR, Al AR, Bi K, Virkud YV, LaFleur MW, et al. Subsets of exhausted CD8(+) T cells differentially mediate tumor control and respond to checkpoint blockade. Nat Immunol. 2019;20(3):326–36.
30. Han Q, Xu L, Lin W, Yao X, Jiang M, Zhou R, et al. Long noncoding RNA CRCMSL suppresses tumor invasive and metastasis in colorectal carcinoma through nucleocytoplasmic shuttling of HMGB2. Oncogene. 2019;38(16):3019–32.
31. Zhao L, Wang H, Liu C, Liu Y, Wang X, Wang S, et al. Promotion of colorectal cancer growth and metastasis by the LIM and SH3 domain protein 1. Gut. 2010;59(9):1226–35.

Figures

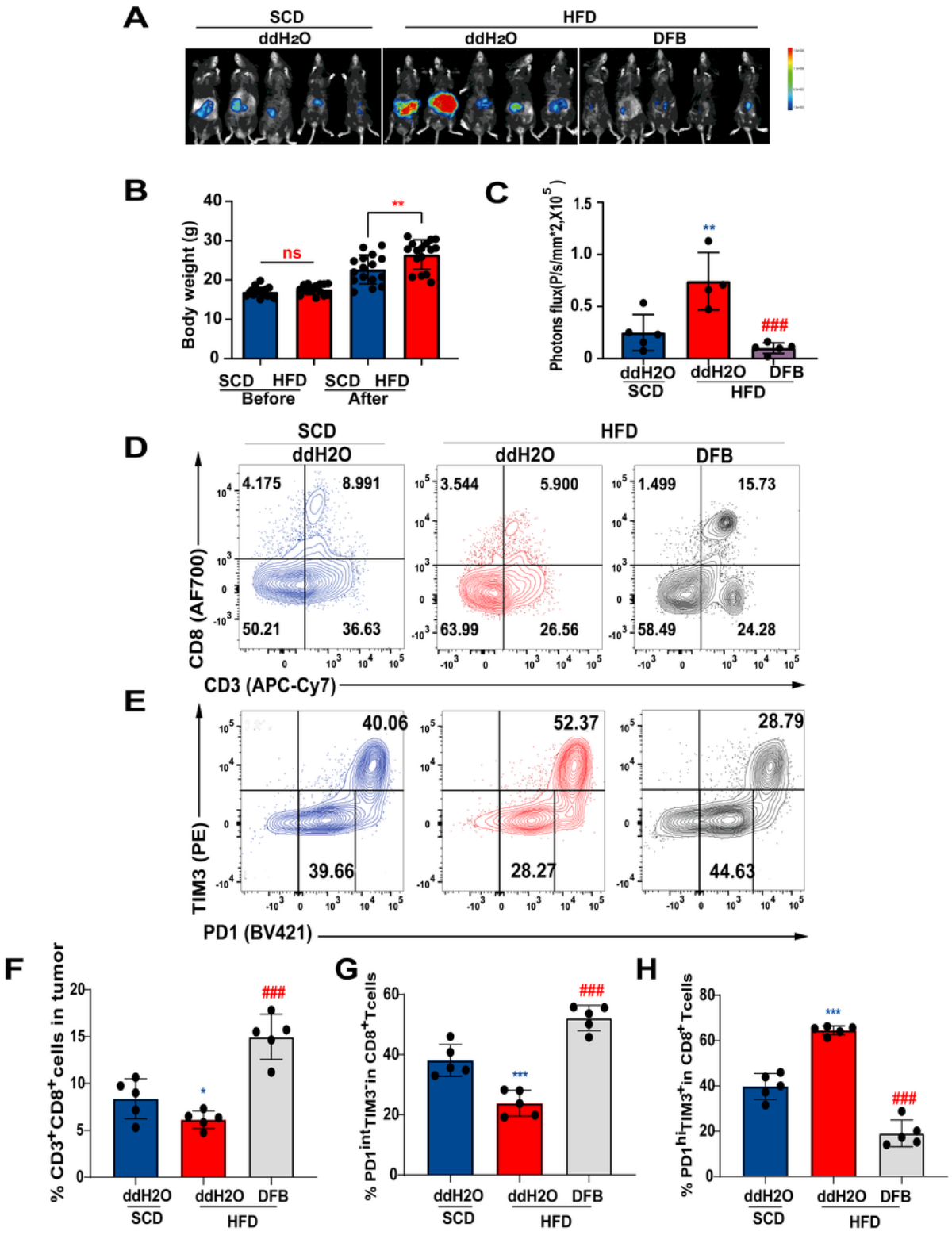

Figure 1

DFB suppresses rapid growth of CRC in DIO mice by restricting terminal Tex. A: In vivo imaging of small animals in the colorectal orthotopic model; B: Body weights of 8 to 16-week-old male control and DIO mice (n = 5 per group) ; C: Fluorescence statistics of figure A–D: Representative flow plots and frequency of CD3+ CD8+ in tumor infiltration of mice in each group（Above）; Representative flow plots and frequency of PD1 and TIM3 in tumor infiltration of mice in each group（Below）; E: Statistical chart of the

expression of CD3+ CD8+ in tumor infiltration each group of mice (n = 5 per group); F: Statistical chart of the expression of PD1mid TIM3- and PD1hi TIM3+on the tumor-infiltrating CD8+ T cells of each group of mice(n = 5 per group). Compared with SCD（ddH2O）group *P ＜ 0.05; **P ＜ 0.01;***P ＜ 0.001. Compared with HFD（ddH2O） group # P ＜ 0.05; ##P ＜ 0.01;###P ＜ 0.001.Data in this figure are all depicted as mean ± SEM, with all individual points shown. Ordinary one-way ANOVA P values are shown.

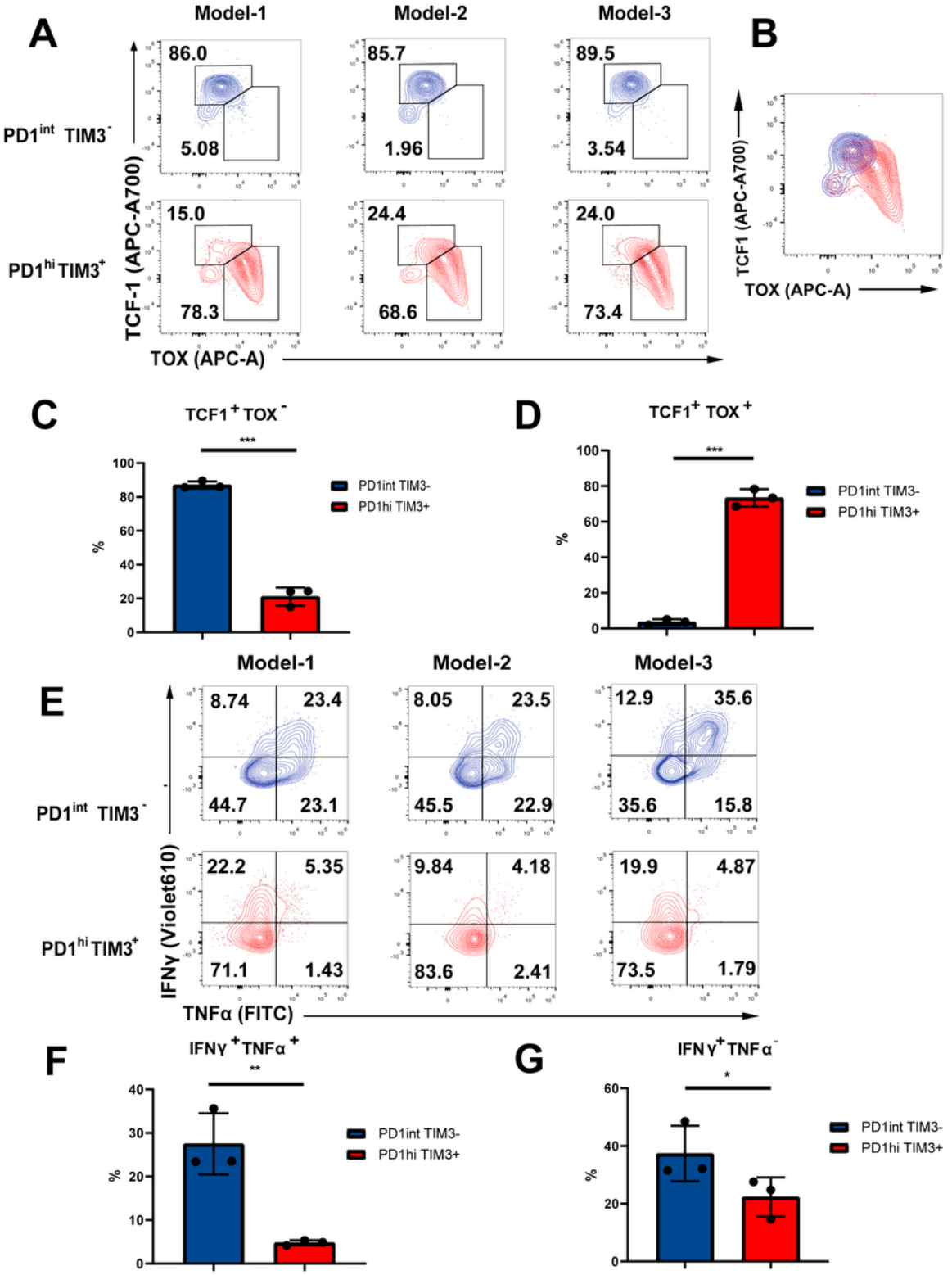

Figure 2

TOX and TCF1 control Tex differentiation status. A: Representative flow plots and frequency of TOX and TCF1 in PD1int TIM3- and PD1hi TIM3+ cells (n = 3 per group). C, D: Statistical chart of A (n = 3 per group). E: Representative flow plots and frequency of IFNγ and TNFα expression among CD8+ TILs after Stimulation 6h with CD3/CD28 antibody and (BD) in PD1int TIM3- and PD1hi TIM3+ cells (n = 3 per group). F: Statistical chart of E (n = 3 per group). Statistical significance was assessed by Student's t test (C-D;F-G. not significant [ns], p > 0.05, * P < 0.05, ** P < 0.01).

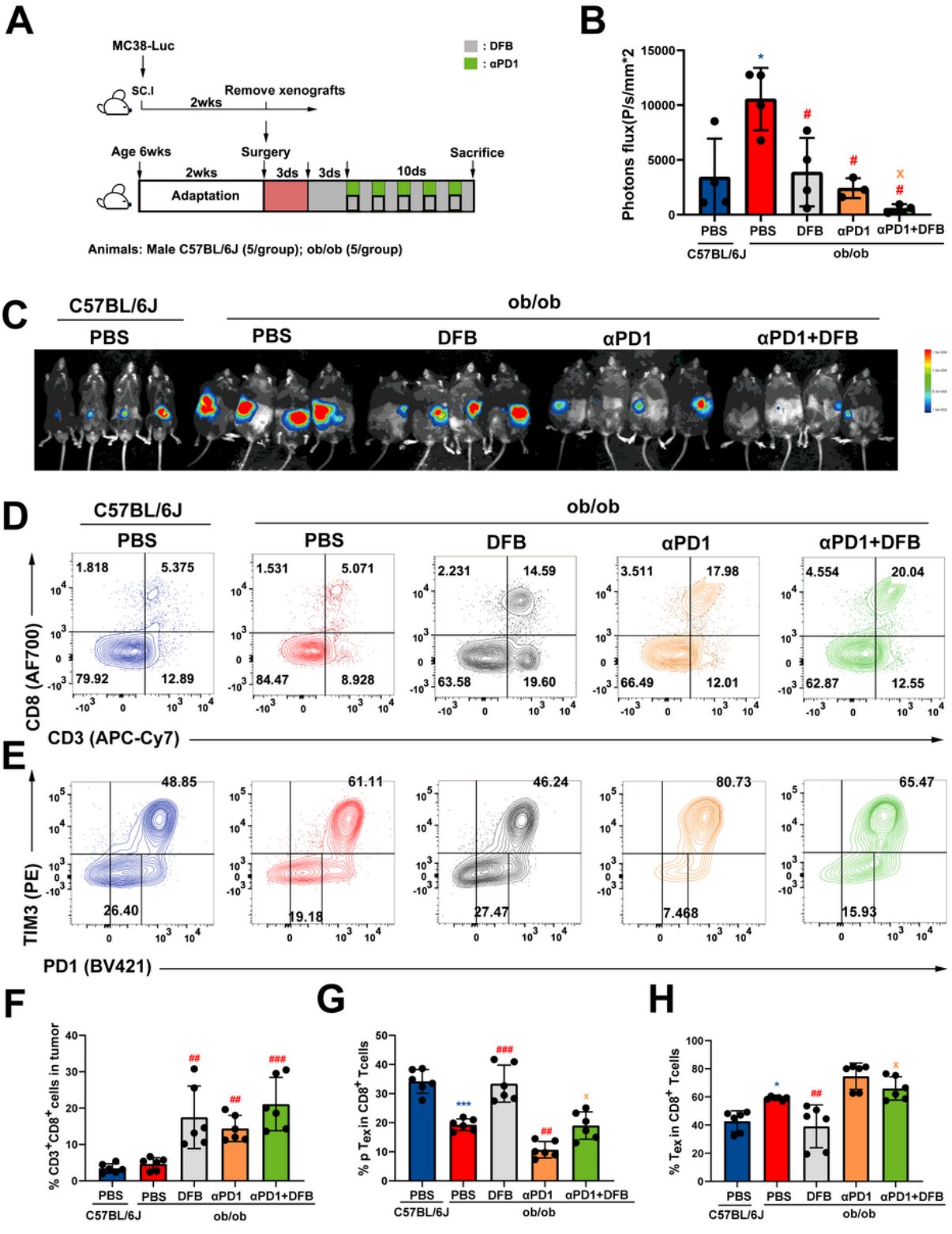

Figure 3

DFB reserves progenitor Tex to elicit immune response to αPD-1. A: Schematic depicting experimental setup. B: Body weights of WT C57BL/6J and ob/ob mice during the experimental. C: In vivo imaging of small animals in the colorectal orthotopic model. D:Representative flow plots and frequency of CD3+ CD8+ in tumor infiltration of mice in each group（Above）; Representative flow plots and frequency of PD1 and TIM3 in tumor infiltration of mice in each group（Below）E: Statistical chart of the expression of CD3+ CD8+ in tumor infiltration each group of mice (n = 5 per group); F: Statistical chart of the expression of t Tex and p Tex on the tumor-infiltrating CD8+ T cells of each group of mice (n = 5 per group). Compared with C57BL/6J（PBS）group, * P ＜ 0.05; ** P ＜ 0.01; *** P ＜ 0.001. Compared with ob/ob（PBS） group, # P ＜ 0.05; ## P ＜ 0.01;### P ＜ 0.001. Compared with ob/ob（αPD1+DFB） group, x P ＜ 0.05.Data in this figure are all depicted as mean ± SEM, with all individual points shown. Ordinary one-way ANOVA P values are shown.

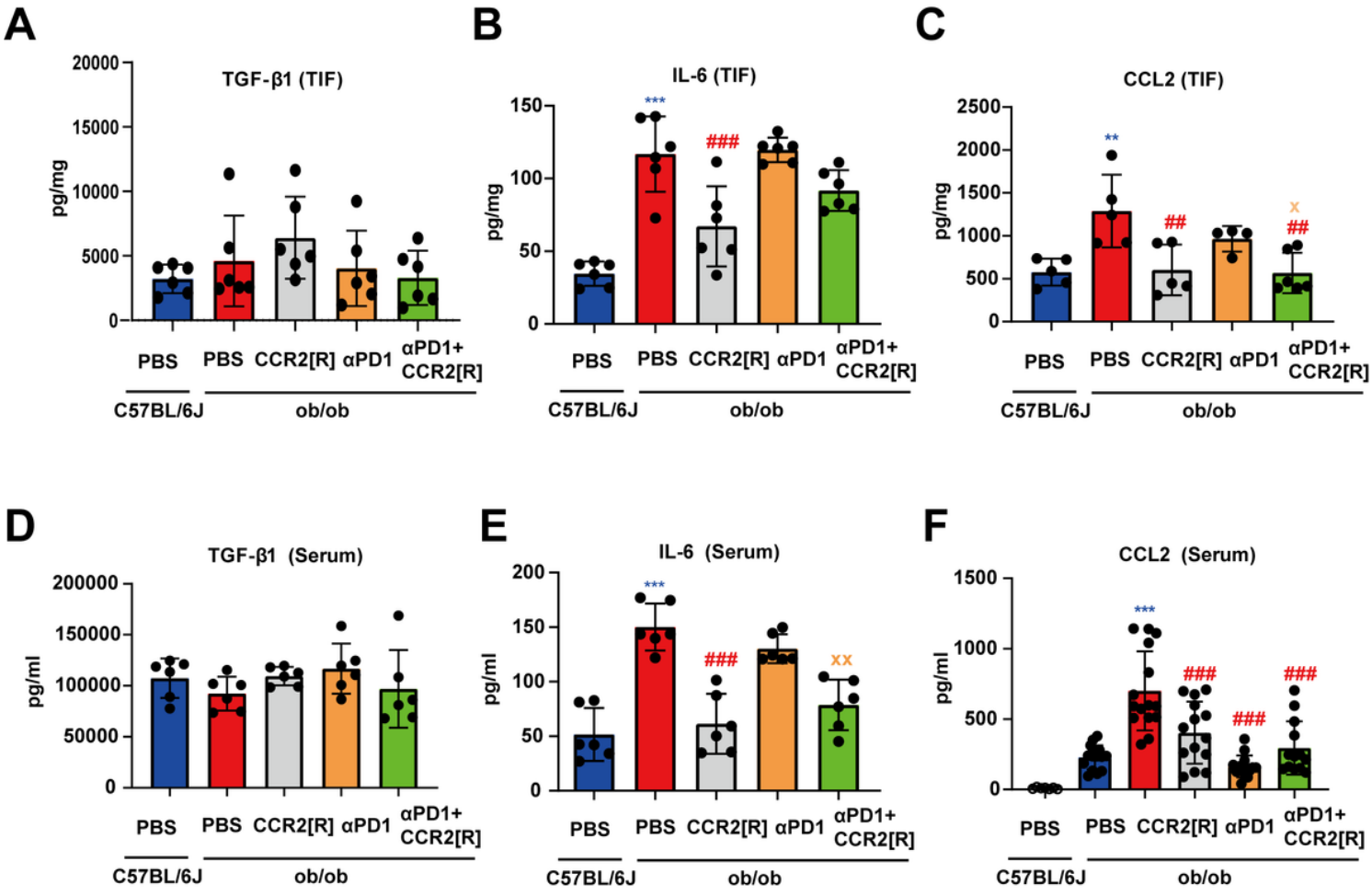

Figure 4

DFB reduces tumor interstitial and serum CCL2 production. Expression of key adipokines in tumor interstitial fluid (TIF) and serum. TGF-β1 in tumor interstitial fluid(A) and serum(D); IL-6 in tumor interstitial fluid(B) and serum(E) ; TGF-β1 in tumor interstitial fluid(C) and serum(F) Compared with C57BL/6J（PBS）group, * P < 0.05; ** P < 0.01; *** P < 0.001. Compared with ob/ob（PBS） group, # P ＜ 0.05; ## P ＜ 0.01;### P ＜ 0.001. Compared with ob/ob（αPD1+DFB） group, xx P ＜ 0.01. Data in this figure

are all depicted as mean ± SEM, with all individual points shown. Ordinary one-way ANOVA P values are shown.

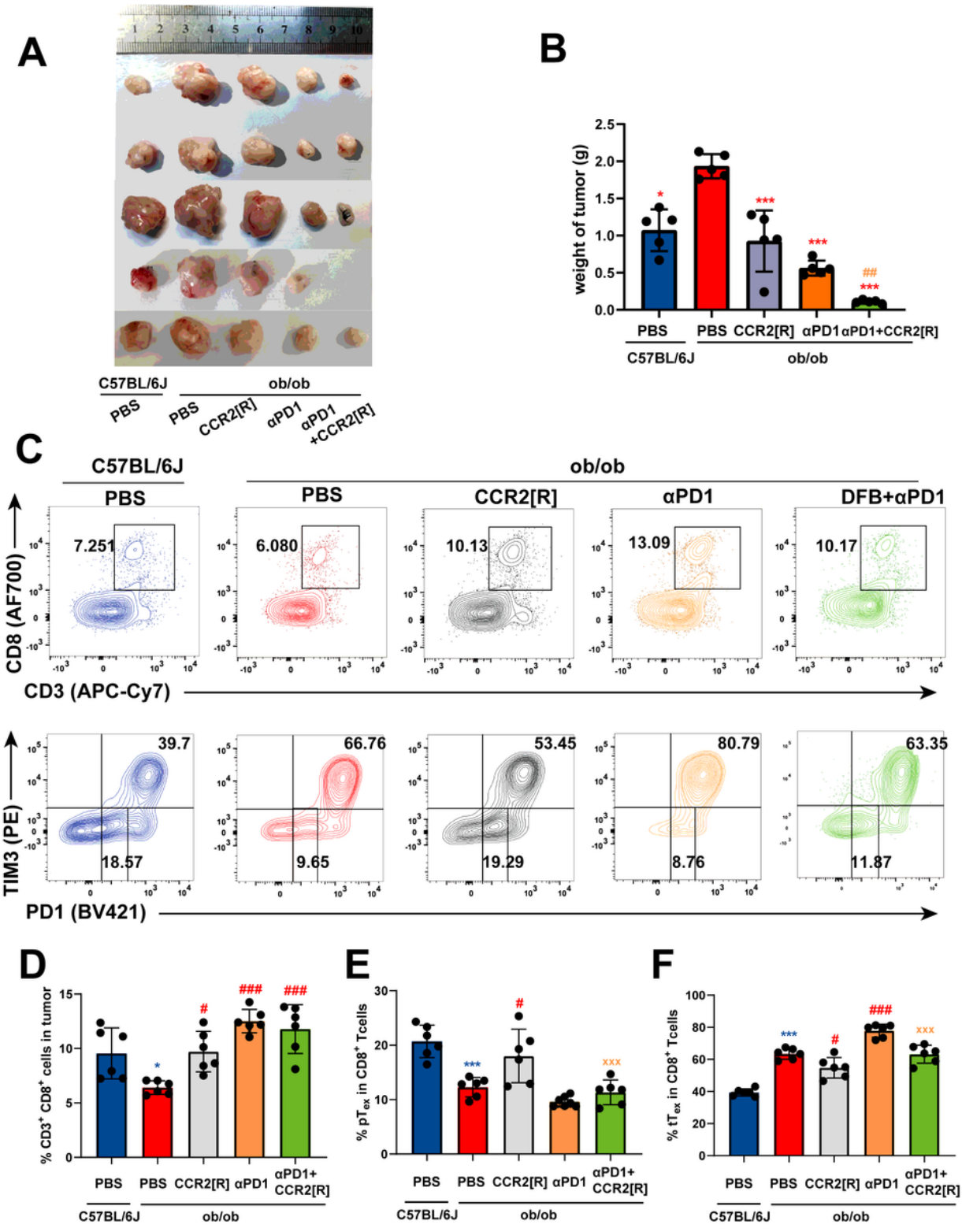

Figure 5

DFB reserves progenitor Tex to elicit immune response to αPD-1. A: Tumor weight of MC38 subcutaneously inoculated in 8-week-old C57BL/6J (n=5) and ob/ob(n=5) male mice. Tumor weight depicted as mean ±SEM. B: Statistical chart of the tumor weight in each group of mice (n = 5 per group).

****P 0.001. C: Representative flow plots and frequency of CD3+ CD8+ in tumor infiltration of mice in each group（Above）; Representative flow plots and frequency of PD1 and TIM3 in tumor infiltration of mice in each group（Below）D: Statistical chart of the expression of CD3+ CD8+ in tumor infiltration each group of mice (n = 5 per group); E: Statistical chart of the expression of t Tex and p Tex on the tumor-infiltrating CD8+ T cells of each group of mice (n = 5 per group). F: Statistical chart of the expression of t Tex and p Tex on the tumor-infiltrating CD8+ T cells of each group of mice (n = 5 per group). Compared with C57BL/6J（PBS）group, * P 0.05; ** P 0.01; *** P 0.001. Compared with ob/ob（PBS） group, # P 0.05; ## P 0.01;### P 0.001. Compared with ob/ob（αPD1+DFB） group, xx P 0.01.Data in this figure are all depicted as mean ± SEM, with all individual points shown. Ordinary one-way ANOVA P values are shown.

Supplementary Files

This is a list of supplementary files associated with this preprint. Click to download.

- SupplementaryMaterial.docx